Compatibility of DSI Implantable Devices with Magnetic Resonance Imaging (MRI)

General Summary

Data were acquired on a Philips Achieva 3.0 Tesla magnet. All images were acquired using the built-in radio frequency (RF) receive "Body" coil. While significant improvement in image quality – specifically the signal to noise ratio (SNR) – can be achieved with the use of specialized coils, it was decided to reduce the potential for damage by limiting the hardware involved in the experiment. A specialized coil would have no advantageous effect on the image distortion produced by the devices.

Displacement Force

The spatial gradient of the magnetic field in the scanner room produces a displacement force on magnetic objects or devices with magnetic components placed in the field. To test displacement force, the object is suspended by a light string (the string is assumed to be massless, so the ratio of string mass to object mass should be very small). While holding the string, the object is moved to the point in the field near the opening of the bore that exerts the greatest deflection. The angular deflection is then recorded and the magnetic force (F_M) calculated by:

$$F_M = mgtan(\theta)$$

Where m is the mass of the object; g is the gravitational acceleration; and θ is the deflection angle. Results are typically expressed in Newtons or as a fraction of the objects gravitational force (F_M/mg). Results for all four devices are shown in Table 1.

Table 1: Displacement Force Exerted on Telemetry Devices

	L21 PTD	D70-PCTR	HD-S21	PA-C10
Object Mass (g)	48	43	7	2
Deflection Angle (◦)	90	90	90	90
Calculated Force (N)	NaN	NaN	NaN	NaN

Unfortunately, due to the extreme deflection angle, the true displacement force could not be calculated (since 90◦ coincides with a vertical asymptote on the tangent graph). The displacement force due to the magnetic field is *much* greater than the gravitation force exerted on each device.

MR Image Acquisition Parameters

There are numerous kinds of acquisitions possible with MRI and it was impractical to experiment with every combination of parameters. The acquisition used – T2 Weighted Turbo Spin Echo sequence – was chosen because: 1) it is very common in clinical/research practice, 2) being a spin echo-based technique, the off-resonance induced on the spins by the presence of the metallic devices could potentially be

refocused by the refocusing radio-frequency pulse, meaning the image artifacts will be less severe than in a gradient echo acquisition and 3) the radio-frequency duty cycle is high, meaning that there is a relatively high amount of radio-frequency (non-ionizing) radiation emitted.

Table 2 Acquisition parameters for the MR data.

Parameter	Value	Parameter	Value
Scan Type	Turbo Spin Echo	Repetition Time (TR)	3000 ms
Av. RF power	78.68877 W	Echo Time (TE)	80 ms
Turbo Spin Echo factor	15	Flip Angle	90°
Pixel BW	193.9 Hz	Refocus Control	120°

Devices were implanted beneath the skin of either a chicken breast (HD-S21 and PA-C10) or a turkey (L21 PTD and D70 PCTR) for MR scanning. The poultry phantom was then placed next to a bottle containing a commonly used solution of water, copper sulfate, and sodium chloride.

Results

Figures 1-4 show sample images from the MR data collected from poultry phantoms with the telemetry devices implanted. In all cases, there is extreme signal loss and image distortion around the implant location. In some cases, the metallic artifacts affect nearly the entire 3D dataset. Note that in Figure 2, the entire chicken breast lacks a signal due to the PA-C10 implant.

Furthermore, each of the devices was subject to displacement while "implanted" under the poultry skin. Further investigation into the amount of force exerted on the muscle tissue should be conducted in coordination with a veterinarian.

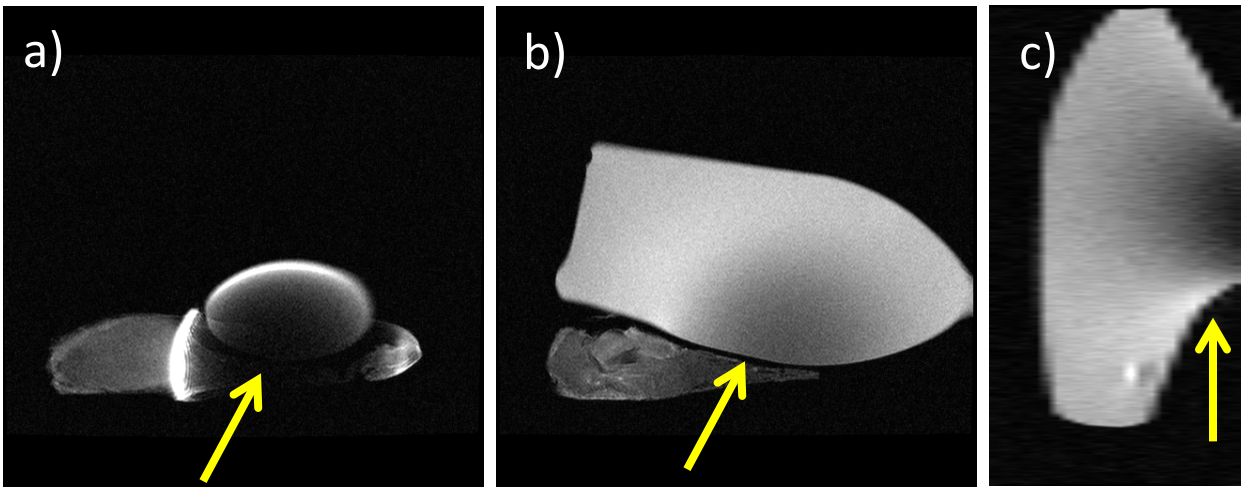

Figure 1: a) Axial slice through chicken breast and solution bottle near the implant location of HD-S21. b) Axial slice through chicken breast and solution bottle superior to implant location. c) Single coronally-reformatted slice through the solution bottle. Image artifacts are highlighted with yellow arrows.

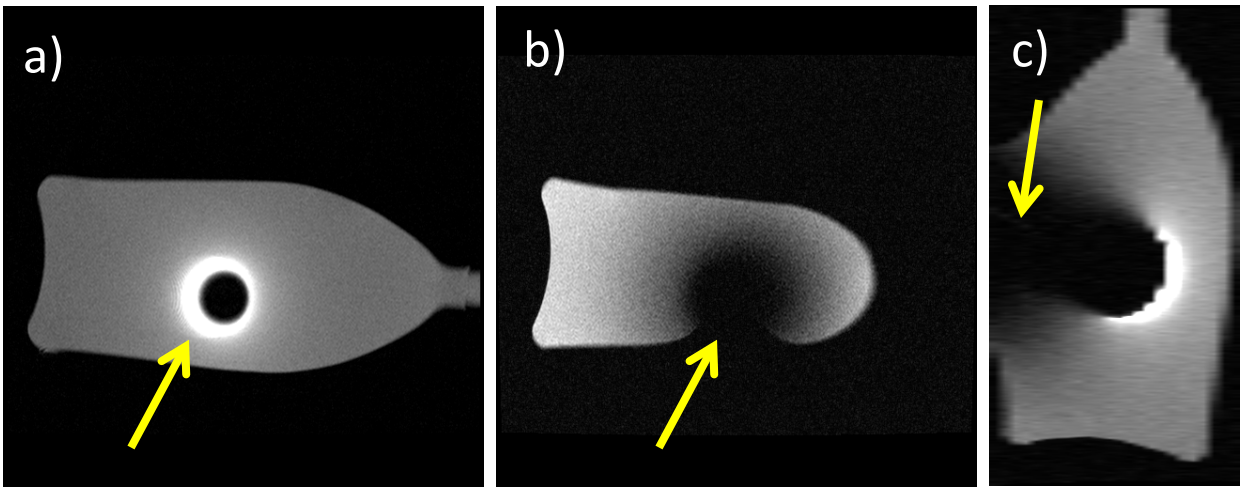

Figure 2: a) Axial slice through chicken breast and solution bottle near the implant location of HD-S21. b) Axial slice through chicken breast and solution bottle superior to implant location. c) Single coronally-reformatted slice through the solution bottle. Image artifacts and geometrical distortion are highlighted with yellow arrows.

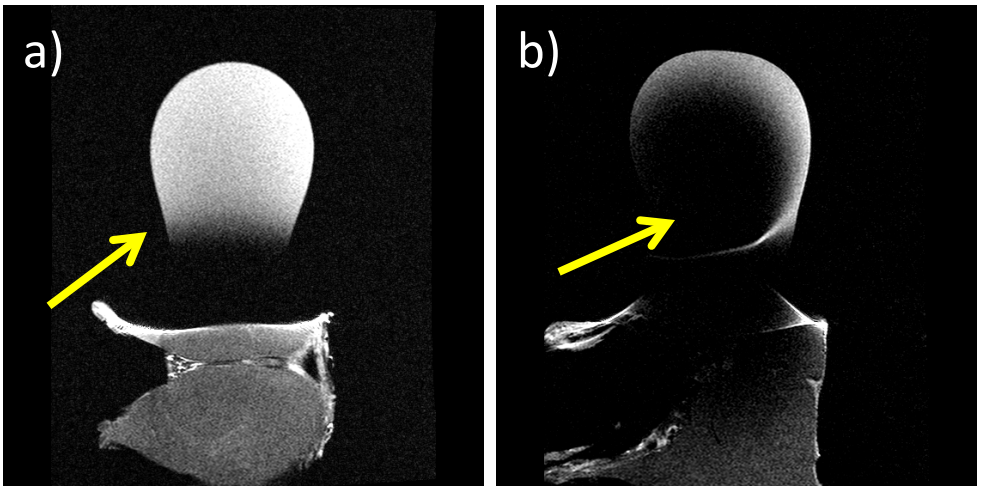

Figure 3: Oblique slices through the turkey and solution bottle with D70 PCTR device. Image artifacts and geometrical distortion are highlighted with yellow arrows.

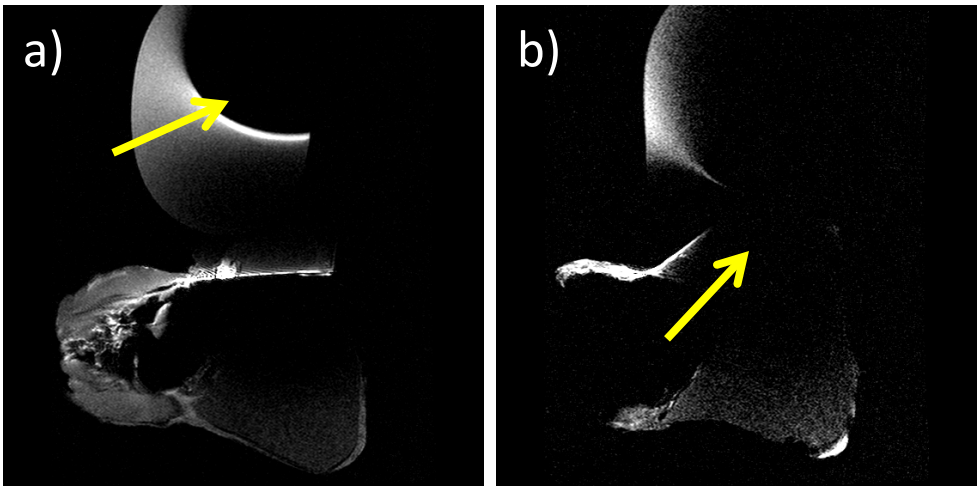

Figure 4: Oblique slices through turkey and solution bottle with L21 PTD device. Image artifacts and geometrical distortion are highlighted with yellow arrows.

Impact of DSI Implantable Devices on Computed Tomography (CT) Images

CT Image Acquisition Parameters

Data were acquired on a Philips Brilliance 16 slice CT scanner.

Table 3: Acquisition parameters for the CT data

Parameter	Value
Tube Voltage*	140 kVp
Tube Current	272 mA
Slice Thickness	0.8 mm
Slice Spacing	0.4 mm
In-Plane Resolution	0.98 x 0.98 mm

*Tube voltage determines the maximum photon energy of the emitted photon energy spectrum. 140 kVp corresponds to a maximum photon energy of 140 Kev, which is the maximum setting for the Phillips Brilliance CT scanner.

Results

Figures 5-7 show axial cross-sections through each of the DSI devices that were scanned. The same cross-section is shown with three different image display settings. Two settings are typically used clinically for lung and abdomen imaging (a and b, respectively) while the third setting is used to demonstrate the extent of the streak artifact. Note that while the source of the artifact is small, the artifacts themselves will permeate the entire axial cross section. The apparent severity of the artifacts will vary depending on the image display settings required for a given exam.

Figure 8 shows a single slice of a coronal reformation of the axially collected data. This figure illustrates the limited extent of the streak artifact in the superior/inferior direction (yellow brackets). This concept is further illustrated in Figure 9, which shows a drawing of an intra-abdominally implanted L21 PTD in a non-human primate. The red shaded box indicates the axial cross-sections that will be most severely degraded by streak artifacts. Chest and head anatomy cross-sections will not affected by the device. However, biopotential leads will cause some streak artifact, though not as severely as the device itself.

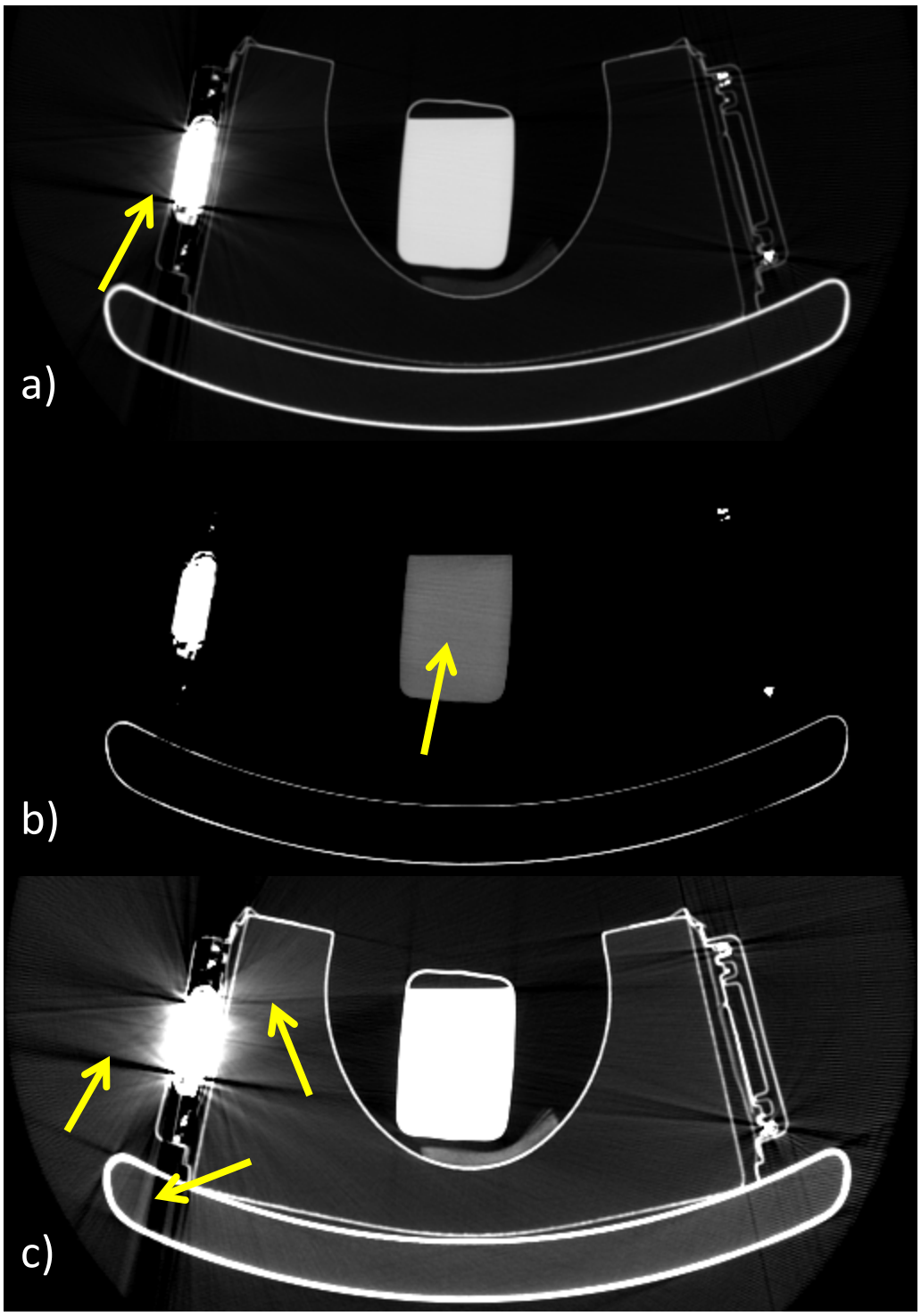

Figure 5: Axial cross-sections of L21 PTD implant are shown with various image display settings. Lung (a) and abdomen (b) display settings are commonly used to view the respective anatomy. (c) uses an image display setting (Level: -866, Width: 314) not commonly used that illustrates the extent of the streak artifact caused by the implant. In all figures, examples of streak artifact are highlighted by yellow arrows.

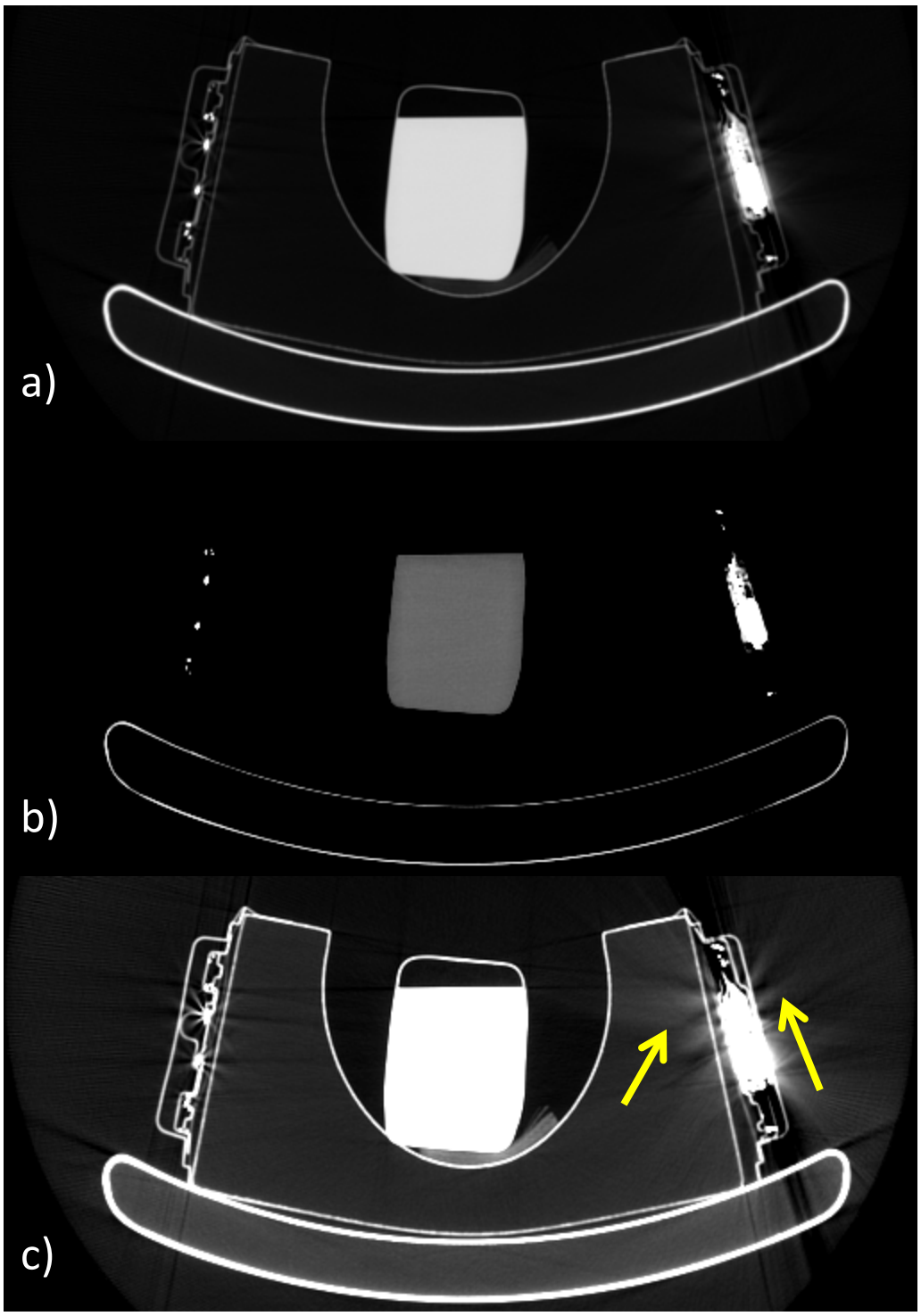

Figure 6: Axial cross-sections of D70 PCTR implant are shown with various image display settings. Lung (a) and abdomen (b) display settings are commonly used to view the respective anatomy. (c) uses an image display setting (Level: -866, Width: 314) not commonly used that illustrates the extent of the streak artifact caused by the implant. In all figures, examples of streak artifact are highlighted by yellow arrows.

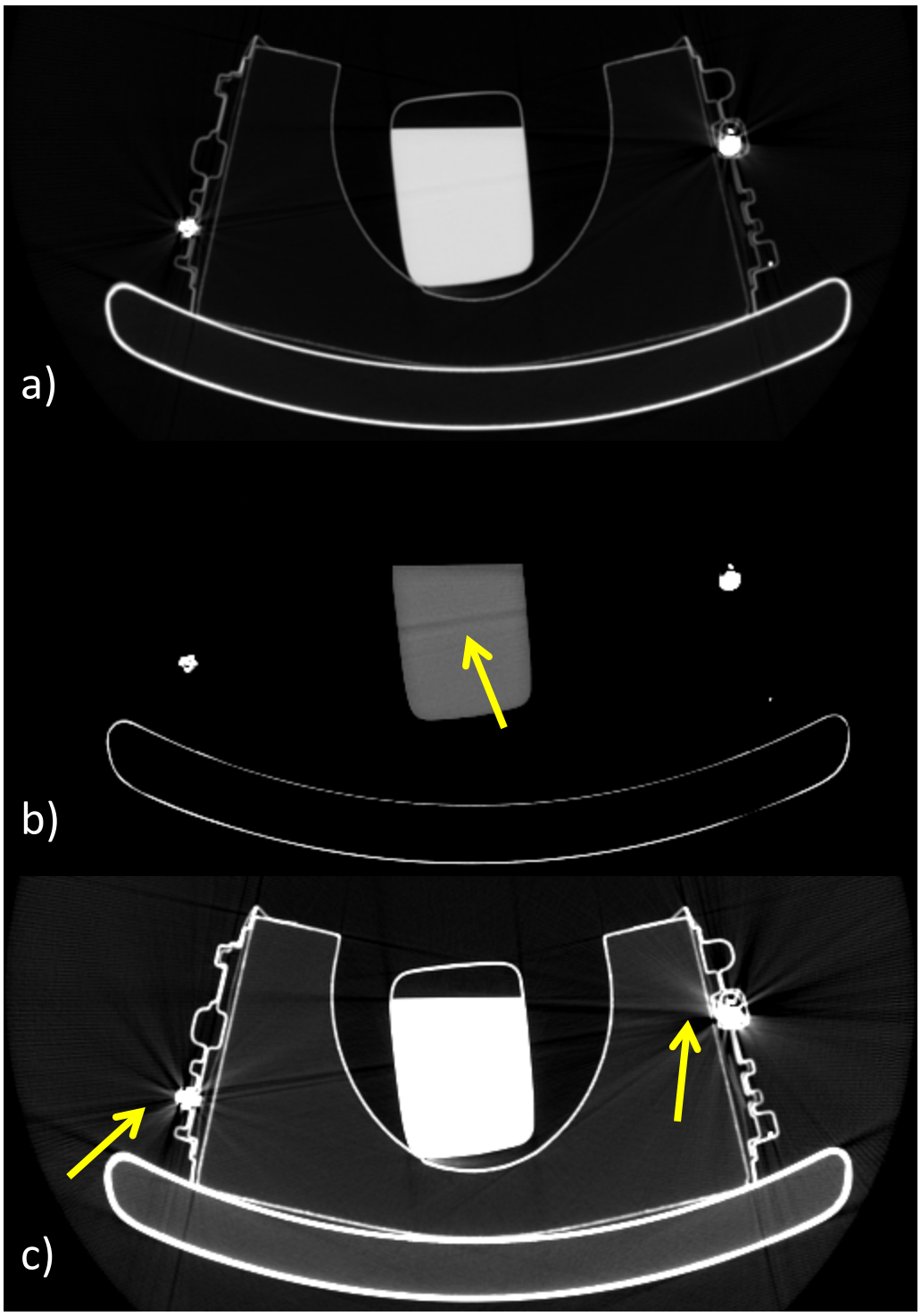

Figure 7: Axial cross-sections of PA-C10 (left) and HD-S21 (right) implant are shown with various image display settings. Lung (a) and abdomen (b) display settings are commonly used to view the respective anatomy. (c) uses an image display setting (Level: -866, Width: 314) not commonly used that illustrates the extent of the streak artifact caused by the implant. In all figures, examples of streak artifact are highlighted by yellow arrows.

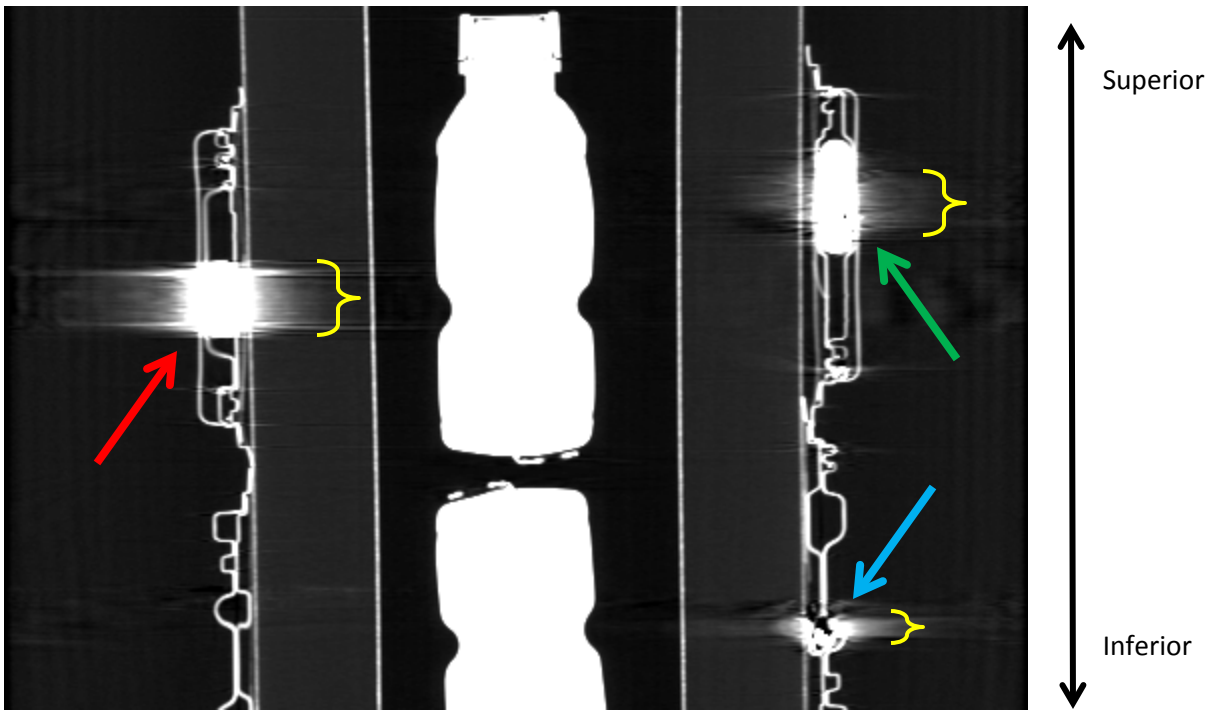

Figure 8: A single slice of a coronal reformation of the acquired CT data is shown. L21 PTD (red arrow) D70 PCTR (green arrow) and HD-S21 (blue arrow) are shown. (The PA-C10 is not included in this slice.)

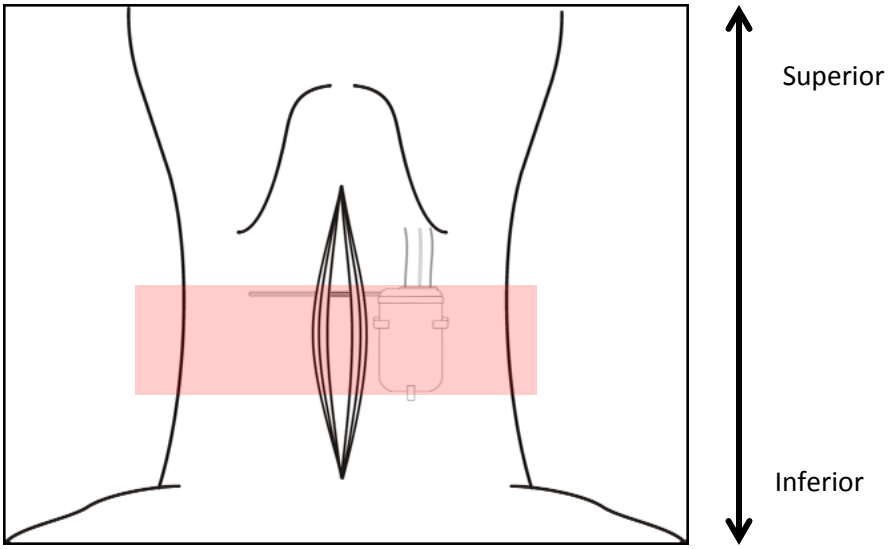

Figure 9: Drawing showing intra-abdominal placement of the L21 PTD device (from PhysioTel Digital Device Surgical Manual). The red shaded box indicates cross-sectional slices that will be most severely degraded due to streak artifact emanating from the device.